XIV International Conference on Computational Plasticity. Fundamentals and Applications
COMPLAS 2019
E. Oñate, D.R.J. Owen, D. Peric , M. Chiumenti, and Eduardo de Souza Neto (Eds)

FINITE ELEMENT ANALYSIS OF TUBE DRAWING PROCESS WITH DIAMETER EXPANSION

SHOHEI KAJIKAWA[*], HIKARU KAWAGUCHI[*], TAKASHI KUBOKI[*], ISAMU AKASAKA[†], YUZO TERASHITA[†] AND MASAYOSHI AKIYAMA[††]

[*] Department of Mechanical Engineering & Intelligent Systems
The University of Electro-Communications
1-5-1 Chofu Gaoka, Chofu-shi, Tokyo, 182-8585, Japan
e-mail: s.kajikawa@uec.ac.jp, www.uec.ac.jp/eng/

[†] Miyazaki Machinery Systems Co., Ltd.
1 Nii, Kaizuka-shi, Osaka, 597-8588, Japan
www.miyazakijp.com

[††] Akiyama Mechanical Engineering Consulting
2-7-306 Tanaka Sekiden-cho, Sakyo-ku, Kyoto-shi, Kyoto, 606-8203, Japan

Key words: Drawing, Flaring, Tube expansion, Thickness reduction, FEM.

Abstract. This paper presents a tube drawing process with diameter expansion for producing a thin-walled tube effectively. In this proposed process, the tube was flared by a plug pushing into the tube, and then the tube was expanded by drawing the plug in the tube axial direction with chucking the flared tube edge. Optimum plug shape, such as the plug half angle and the corner radius, was investigated by a series of analyses using the finite element method (FEM) for improving the forming limit and the dimension accuracy. At first, a friction coefficient was determined to 0.3 by a comparison of the flaring limit between the analysis and the experiment of the tube flaring. As a result of the analyses in the drawing with the diameter expansion, the forming limit was high when the plug half angle was set to 18~30°. The thickness reduction ratio increased with an increase in the expansion ratio and the plug half angle. In addition, the overshoot, which is a difference between the plug diameter and the tube inner diameter after the drawing, was prevented by using the plug with the corner radius of 20 mm.

1 INTRODUCTION

Drawing process is conventionally applied for manufacturing tubes for reducing thickness and improving dimensional accuracy and strength. The tubes, which is manufactured by the drawing, is used for various machine and construction components, such as plumbing equipment, constructional material and so on. There are many research works for the tube drawing. For example, Kuboki et al. proposed methods for levelling residual stress, and reducing thickness variation in the tube drawing [1, 2].

In recent years, thin-walled tubes, which contribute to reduction in size and weight of various machine components, are required for environmental protection. However, typical thickness

reduction is about 20 % in 1 pass drawing [3]. Therefore, many drawing passes are required for manufacturing thin-walled tubes from rather thick-walled raw tubes, and the production cost increases with the increase of the number of the drawing passes. Another method for manufacturing thin-walled tube is pilgering [4]. Area reduction is over 80 %, but productivity and dimensional accuracy is low compared to the drawing, because the pilgering is an incremental processing. Furushima et al. proposed dieless drawing, which contributes to the large area reduction in 1 drawing pass [5]. However, the tubes, which are manufactured by the dieless drawing, are unsuitable for machine component which requires the dimensional accuracy. Therefore, effective processing method should be developed for manufacturing the thin-walled tube.

2 TUBE DRAWING PROCESS WITH DIAMETER EXPANSION

This paper proposed a tube drawing process with a diameter expansion as shown in Figure 1. The proposed method is composed of two steps. In the first step which is tube flaring, the tube edge is expanded by pushing the plug into the tube as shown in Fig. 1 (a). In second step which is the plug drawing, the tube is expanded through the whole tube length by drawing the plug while the flared portion is chucked as shown in Fig. 1 (b).

The advantage of the proposed method is the effective production of the thin-walled tube. Figure 2 shows the comparison of stress state between the conventional and the proposed method. In the case of the proposed method, the tube wall is stretched in both of the axial and the hoop directions, then a negative deviatoric stress is large in the thickness direction, with

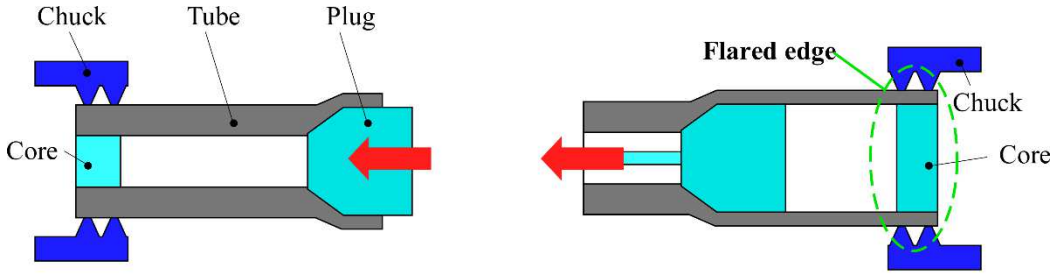

(a) Flaring (1st steps) (b) Drawing (2nd step)

Figure 1: Schematic diagram of tube drawing process with diameter expansion

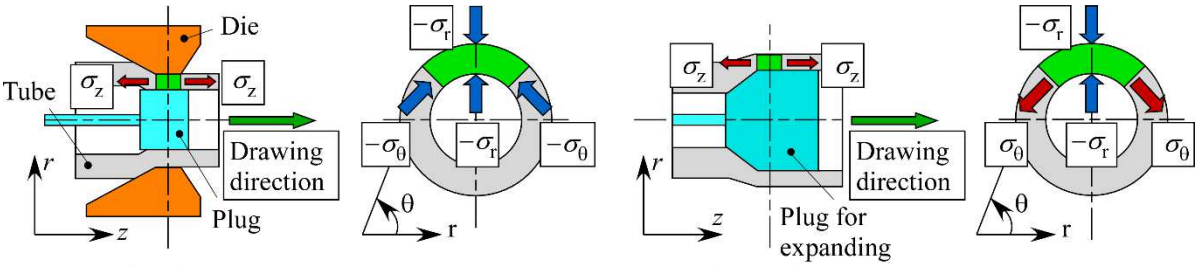

(a) Drawing with shrink（Conventional method） (b) Drawing with expansion（Proposed method）

Figure 2: Comparison of stress state between drawing with shrink and expansion

compared to that of the conventional tube drawing with diameter shrinkage. Thus, the proposed method is considered to be effective for reducing the thickness of the tube.

In this study, optimum plug shape, such as the plug half angle and the corner radius, was investigated for improving the forming limit and the dimension accuracy. At first, the tube flaring, which is 1st step, was carried out in the experiment and the analysis by finite element method (FEM), and the friction coefficient μ was estimated by comparison of the flaring limit between the experiment and the FEM. In drawing process, which is 2nd step, a series of the analyses were carried out for identifying the optimum plug shape.

3 INVESTIGATION IN FLARING PROCESS

3.1 Flaring method and conditions

An elastic-plastic analysis by the FEM was carried out by using the commercial code "ELFEN" which was developed by Rockfield Software Limited, Swansea. Figure 3 shows the schematic diagram of the model for the tube flaring. The model is two dimensional with axisymmetry. The von Mises yield criterion was adopted, and normality principle was applied to the flow rule. The constraints were determined by the penalty function method, and an implicit scheme was adopted. Four-node rectangular elements were adopted. The F-bar method was applied to the element for overcoming volumetric locking [6].

In the analysis of the tube flaring, one tube edge was flared by the plug pushing, while the other edge was fixed in the axial direction and the outer surface was held by the holder. The

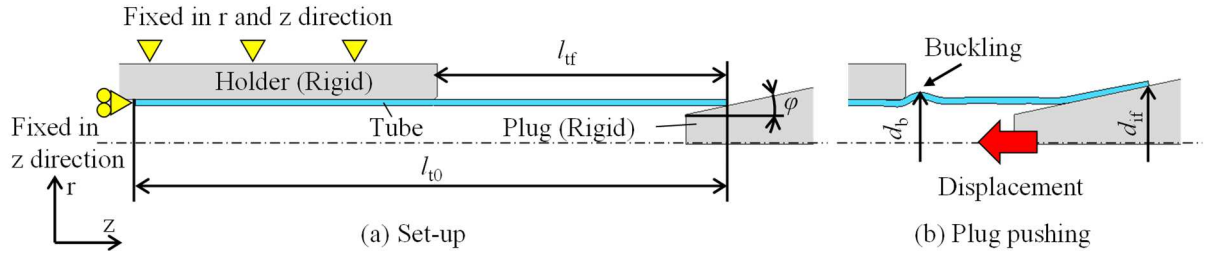

Figure 3: Schematic diagram of FEA model for tube flaring

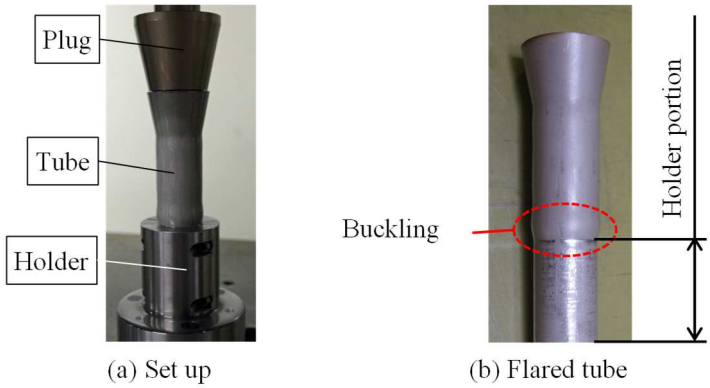

Figure 4: Appearance of experimental set-up and flared tube

Table 1: Working conditions in flaring process

Tube	Tube material	SUS304	
	Swift's equation of SUS304 (FEM)	σ=1275(ε_p+0.01)$^{0.39}$	
	Initial diameter d_0 [mm]	30	
	Initial thickness t_0 [mm]	1, 2, 3, 4	
	Initial length l_{t0} [mm]	200	
	Initial flared length l_{tf} [mm]	100	
	Element size (FEM)	Axial	1 mm/division
		Radial	8 divisions
Plug	Half angle φ [°]	12, 24, 36, 48	
Friction coefficient μ (FEM)		0.1, 0.2, 0.3, 0.4	
Lubrication (Experiment)		With lubricant	

flaring ratio E_f was defined as the following equation.

$$E_f = \frac{d_{if} - d_{i0}}{d_{i0}} \tag{1}$$

where d_{if} is the inner diameter at the flared edge, and d_{i0} is the initial inner diameter. The buckling occurred as a defect by the plug pushing as shown in Fig. 3 (b). The buckling amount B was defined as the following equation.

$$B = \frac{d_b - d_0}{d_0} \tag{2}$$

where d_b was the outer diameter of the buckling portion, and d_0 was the initial outer diameter. Maximum flaring ratio E_{f_max}, which means flaring limit, was defined as the maximum value of E_f before B reaching 0.05. The experiments were carried out in a similar way to FEM as shown in Figure 4. d_{if} and d_b were measured every 2 mm of the plug pushing in the axial direction.

Table 1 shows the working conditions for the tube flaring in the FEM and the experiment. The tube material was SUS304, and thickness t_0 was from 1 to 4 mm. Plugs with various half angle φ, which were from 12 to 48°, were prepared. The experimental results were compared to the FEM results with various friction coefficient μ.

3.2 Maximum flaring ratio

Figure 5 shows the effect of the tube initial thickness t_0 on the maximum flaring ratio E_{f_max} when the plug half angle φ was 12°. E_{f_max} increased with an increase in t_0. In addition, E_{f_max} was higher under the condition of the low friction coefficient μ in FEM results. This is because the axial load, which causes buckling occurrence, decreases with the decrease in the frictional force. The experimental results almost agreed with the FEM result of μ=0.3.

Figure 6 shows the effect of the plug half angle φ on the maximum flaring ratio E_{f_max} when the tube initial thickness t_0 was 2 mm. E_{f_max} was low under the condition of low φ because the frictional force was high due to the large contact area at the plug taper portion. On the other hand, E_{f_max} was also low when φ was too large, because the axial load was high due to the large bending/unbending deformation of the tube wall. Therefore, the optimum φ was ranged from

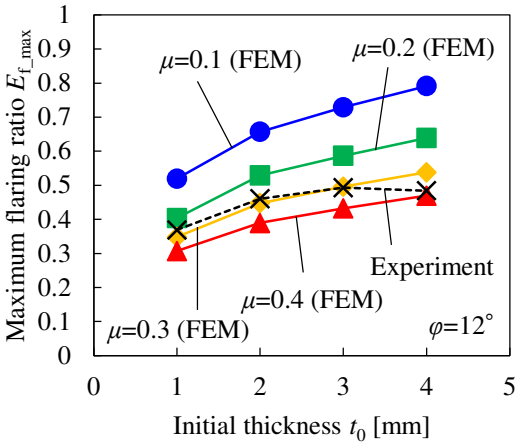

Figure 5: Effect of tube initial thickness t_0 on maximum flaring ratio E_{f_max} (Plug half angle φ=12°)

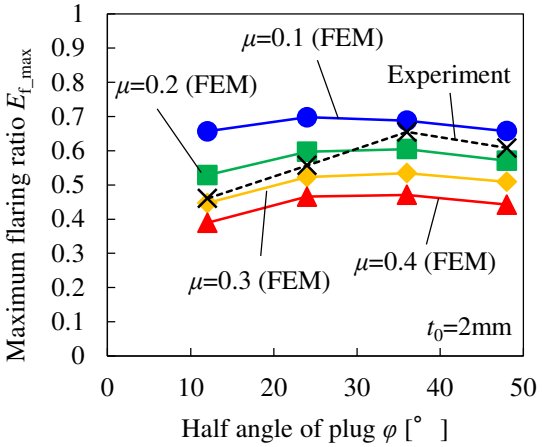

Figure 6: Effect of plug half angle φ on maximum flaring ratio E_{f_max} (Tube initial thickness t_0=2 mm)

24 to 36°.

The experimental results agreed with the FEM result of the friction coefficient μ=0.3 when the plug half angle φ was 12~24°, but the experimental results were ranged from 0.1 to 0.2 of μ in FEM results when φ was 36~48°. It was considered that the lubrication state changed by φ in the experiment. Oil film, which is between the tube wall and the plug, is easy to be lost when the sliding length is long with the low φ in the experiment. In addition, the tube wall waved at the taper portion under the condition of high φ [7]. The waved tube wall did not contact to the plug and held the lubricant in the experiment. Therefore, it was considered that μ which the experimental results agreed with the FEM results decreased with the increase in φ. Base on the results as shown in Fig. 5 and 6, μ was set to 0.3 for the analysis of the drawing process, which is described in the next section, in order to estimate the forming limit in safety.

4 INVESTIGATION IN DRAWING PROCESS

4.1 Drawing method and conditions

Figure 7 shows the schematic diagram of the FEM model for the drawing process. The plug was drawn into the tube, while one tube edge was fixed in the axial direction. Expansion ratio E_d, thickness reduction ratio γ and dimensional accuracy were evaluated. E_d was defined as the following equation.

$$E_d = \frac{d_i - d_{i0}}{d_{i0}} \tag{3}$$

where d_i is the tube inner diameter after the plug drawing, and d_{i0} is the initial tube inner diameter. γ was defined as the following equation.

$$\gamma = \frac{t - t_0}{t_0} \tag{4}$$

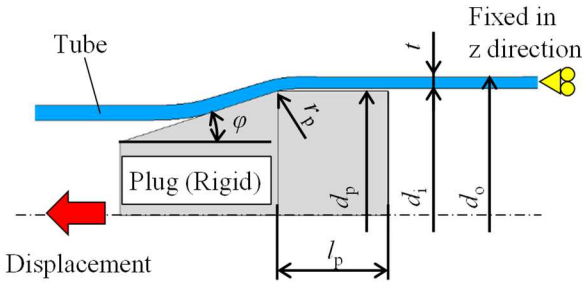

Figure 7: Schematic diagram of FEM model for drawing process

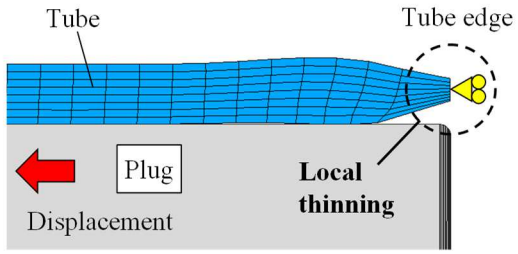

Figure 8: Appearance of local thinning (Tube initial thickness t_0=2 mm, plug half angle φ=18° , Plug diameter d_p=45 mm, plug corner radius r_p=0 mm)

Table 2: Working conditions in drawing process

Tube	Tube material		SUS304
	Swift's equation of SUS304		σ=1275(ε_p+0.01)$^{0.39}$
	Initial diameter d_0 [mm]		30
	Initial thickness t_0 [mm]		1, 2, 3, 4
	Initial length l_{t0} [mm]		200
	Element size	Axial	1 mm/division
		Radial	8 divisions
Plug	Straight length l_p [mm]		15
	Half angle φ [°]		6, 12, 18, 24, 30, 36
	Diameter d_p [mm]		30~47.5
	Corner radius r_p [mm]		0, 10, 20, 30
Friction coefficient μ			0.3

where t is the thickness after the plug drawing, and t_0 is the initial thickness. The dimensional accuracy was evaluated by overshoot δ, which means the difference between d_i and d_p. δ was defined as the following equation.

$$\delta = d_i - d_p \tag{5}$$

Table 2 shows the working conditions in drawing process. The tube initial thickness t_0, the plug diameter d_p, half angle φ and corner radius r_p were changed variously. When d_p was too high in each t_0 and φ, a local thinning occurred at the tube edge, which is fixed in the axial direction, as shown in Figure 8. Maximum expansion ratio E_{d_max} was defined as the maximum value of the expansion ratio E_d when the plug was drawn without the local thinning. E_{d_max} was searched by increasing d_p in the step of 0.5 mm until the local thinning occurred.

4.2 Effect of plug half angle on expansion ratio and thickness reduction

Figure 9 shows the effect of the plug half angle φ and the tube initial thickness t_0 on maximum expansion ratio E_{d_max}. E_{d_max} increased with an increase in φ, and E_{d_max} was higher when φ was 18~30 °. However, E_{d_max} decreased when φ was over 30°. Forming limit was considered to be determined by the drawing load P. Figure 10 shows the effect of φ on the

drawing load P in each d_p. P was higher under the condition that φ was too low or high. In the case that φ was too low, P became high due to the large frictional force, which is derived from the large contact area at the plug taper portion. In the case that φ was too high, P was higher because bending/unbending deformation became large by increasing φ. Optimum φ, which decreases P, increased with the increase in d_p, and the optimum φ was 24° when d_p was 42 mm, which was near the forming limit. This value of φ was same as φ when E_{d_max} was the highest in Fig. 9. This result suggested that P should be decreased by controlling φ appropriately for improving the forming limit.

Figure 11 shows the effect of the plug half angle φ and tube initial thickness t_0 on maximum thickness reduction ratio γ_{max}. γ_{max} is the thickness reduction ratio γ when the expansion ratio E_d was the maximum E_{d_max}. γ_{max} increased drastically with the increase in φ when φ was 6~18°,

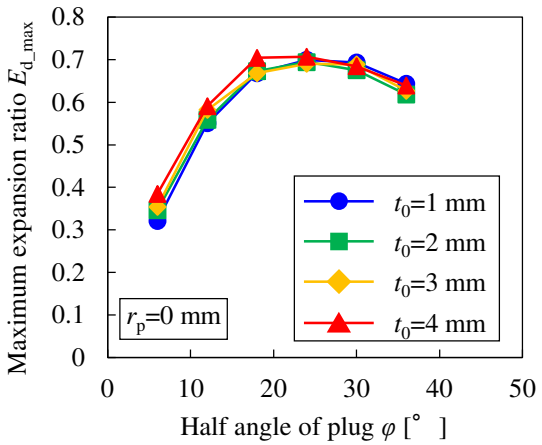

Figure 9: Effect of plug half angle φ and tube initial thickness t_0 on maximum expansion ratio E_{d_max} (Plug corner radius r_p=0 mm)

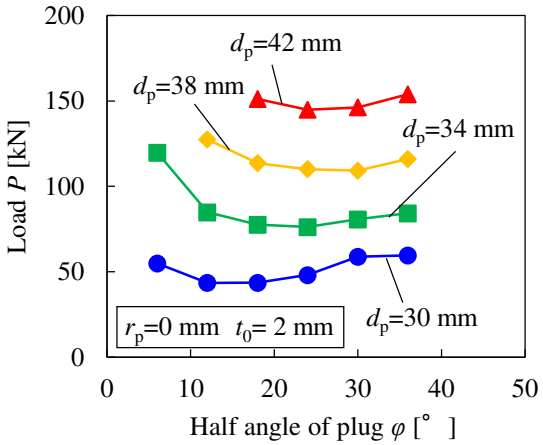

Figure 10: Effect of plug half angle φ and plug diameter d_p on drawing load P (Tube initial thickness t_0=2 mm, plug corner radius r_p=0 mm)

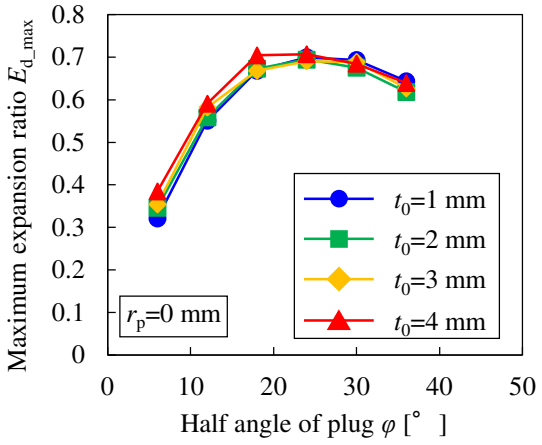

Figure 11: Effect of plug half angle φ and tube initial thickness t_0 on maximum thickness reduction ratio γ_{max} (Plug corner radius r_p=0 mm)

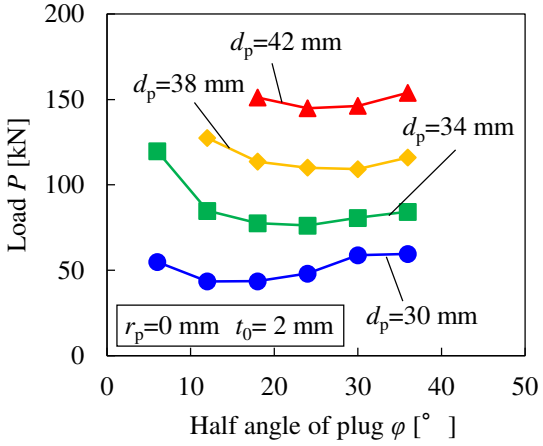

Figure 12: Effect of plug half angle φ and plug diameter d_p on thickness reduction ratio γ (Tube initial thickness t_0=2 mm, plug corner radius r_p=0 mm)

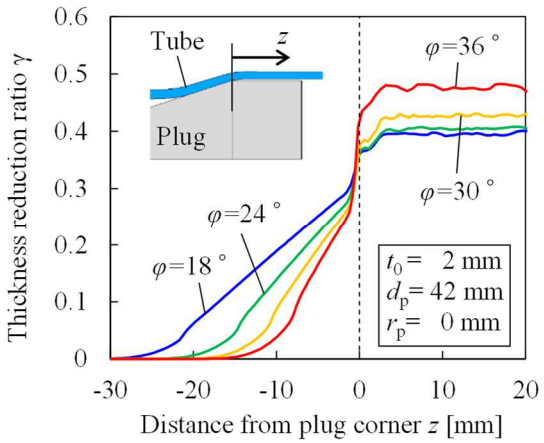

Figure 13: Effect of plug half angle φ on distribution of thickness reduction ratio γ (Tube initial thickness t_0=2 mm, plug diameter d_p=42 mm, plug corner radius r_p=0 mm)

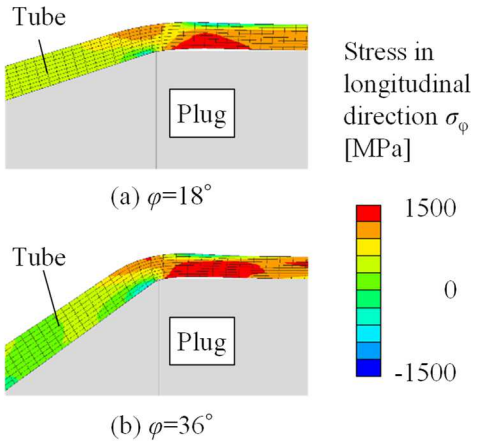

Figure 14: Distribution of stress in logitudinal direction σ_φ (Tube initial thickness t_0=2 mm, plug diameter d_p=42 mm, plug corner radius r_p=0 mm)

and γ_{max} increased gradually with the increase in φ when φ was over 18°, although E_{d_max} decreased with the increase in φ when φ was over 24°. This is because γ increased by increasing φ in each plug diameter d_p, as shown in Figure 12.

Figure 13 shows the effect of the plug half angle φ on the distribution of the thickness reduction ratio γ in the case that the plug diameter d_p was 42 mm. γ increased gradually with the tube expanding at the plug taper portion, and γ increased drastically at the portion near the plug corner. This drastic thickness reduction occurred due to the axial stretching with the bending at the plug corner as shown in Figure 14. The stress in the longitudinal direction σ_φ is large at the plug corner. Therefore, the thickness drastically decreased by stretching the tube wall in the hoop and the axial direction. In addition, γ increased by increasing φ, because σ_φ increased with the increase in φ as shown in Fig. 14 (a) and (b). This result means that the thickness could be controlled by setting φ appropriately.

4.3 Effect of plug corner radius on dimensional accuracy

Figure 15 shows the effect of the plug half angle φ and the expansion ratio E_d on the overshoot δ in the case that the tube initial thickness t_0 was 2 mm, and the plug corner radius r_p was zero. δ decreased with the increase in E_d, but δ increased with the increase in φ. Figure 16 shows the typical appearances of the tube during the plug drawing. When φ and E_d were small, δ was small as shown in Fig. 16 (a). When φ was large with small E_d, δ became large because the bending angle was large as shown in Fig. 16 (b). When φ was large with large E_d, δ became small because the tube wall was stretched strongly in the axial direction due to the large drawing load P, and fit to the plug surface as shown in Fig. 16 (c).

It was considered to be effective to apply the plug with corner radius r_p for improving the dimensional accuracy by preventing the overshoot δ. Figure 17 shows the tube shape during the drawing in the cases that the plug with and without r_p were used. The tube wall was bent with large bending radius, and fit to the plug surface by using the plug with r_p as shown in Fig. 17

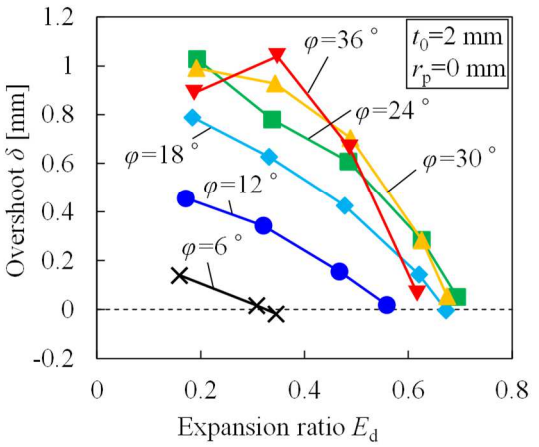

Figure 15: Effect of plug half angle φ and expansion ratio E_d on overshoot δ (Tube initial thickness t_0=2 mm, plug corner radius r_p=0 mm)

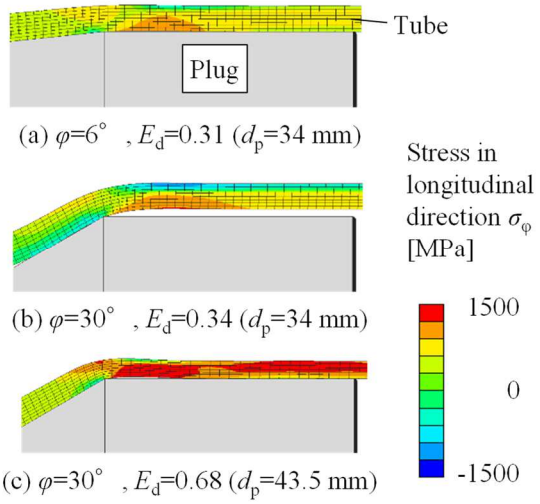

Figure 16: Appearance of tube wall during drawing with diameter expansion (Tube initial thickness t_0=2 mm, plug corner radius r_p=0 mm)

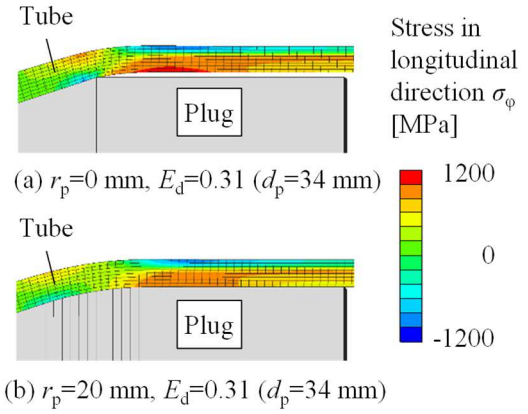

Figure 17: Appearance of tube wall during drawing with diameter expansion (Tube initial thickness t_0=2 mm, plug half angle φ=18°)

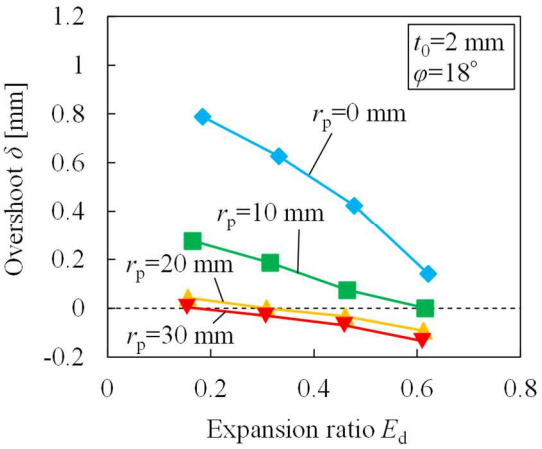

Figure 18: Effect of plug corner radius r_p and expansion ratio E_d on overshoot δ (Tube initial thickness t_0=2 mm, plug half angle φ=18°)

(b). Therefore, δ decreased by applying large r_p to the plug. Figure 18 shows the effect of r_p on δ in the case that the plug half angle φ was 18°. δ decreased with an increase in r_p, and δ was ranged around zero by setting r_p to 20 mm. However, δ was negative value under the condition that E_d was large, such as E_d=0.61. This is because the tube wall shrink in the hoop direction after the plug passing, while the tube wall was stretched strongly in axial direction due to the large drawing load. Figure 19 shows the effect of r_p on δ in the case that φ was 18, 24 and 30°, which was the optimum φ for improving the forming limit as shown in Fig. 9. It was possible to prevent δ by setting r_p to 20 mm regardless of φ.

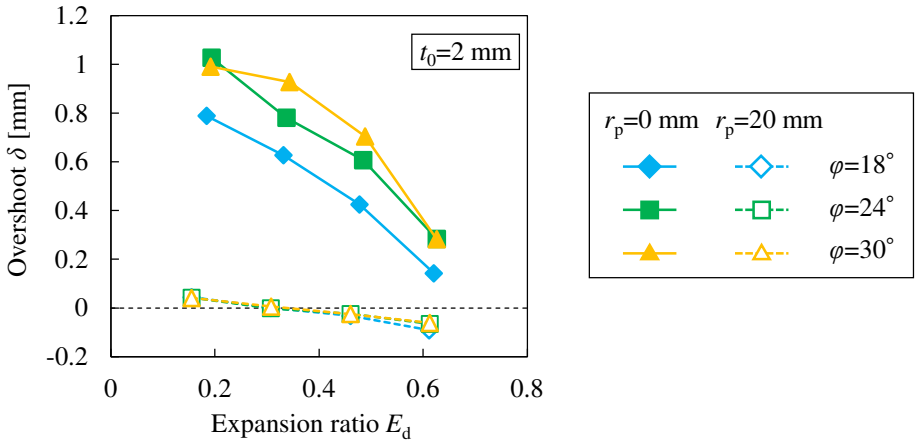

Figure 19: Effect of plug corner radius r_p, plug half angle φ and expansion ratio E_d on overshoot δ (Tube initial thickness t_0=2 mm)

5 CONCLUSIONS

- This paper proposed a tube drawing process with the diameter expansion for producing thin-walled tube effectively, and optimum plug shape, such as the plug half angle φ and the corner radius r_p, was investigated for improving the forming limit and the dimensional accuracy.
- In the tube flaring, the forming limit was higher when the tube initial thickness t_0 was thicker, and the plug half angle φ was 24~36° for improving the flaring limit. The friction coefficient μ was determined to 0.3 by the comparison of the flaring limit between the FEM and the experimental result.
- In the plug drawing, the forming limit was high when the plug half angle φ was set to 18~30°, because the axial load was low during the drawing in this range of φ.
- The thickness reduction ratio γ increased with the increase in the expansion ratio E_d of the tube inner diameter. In the case that E_d was constant, γ became higher by increasing φ.
- The overshoot δ, which is the difference between the plug diameter d_p and the tube inner diameter d_i after the drawing, increased with the increase in the plug half angle φ, and δ changed by the expansion ratio E_d when the plug without the corner radius r_p was used.
- In the case of the plug half angle φ=18~30°, which is the optimum range for improving the forming limit, the overshoot was almost zero regardless of φ and the expansion ratio E_d by using the plug with the corner radius r_p of 20 mm.

REFERENCES

[1] Kuboki, T., Nishida, K., Sakaki and T., Murata, M. Effect of plug on levelling of residual stress in tube drawing. *J. Mater. Process. Technol* (2008) **204**: 162-168.

[2] Kuboki, T., Tasaka and S., Kajikawa, S. Examination of working condition for reducing thickness variation in tube drawing with plug. *Proc. COMPLAS XIV* (2017): 63-71.

[3] The Japan Society for Technology of Plasticity. *Drawing*. Corona Publishing, (2017), in Japanese.
[4] Abe, H., Iwamoto, T., Yamamoto, Y., Nishida and S., Komatsu, R. Dimensional accuracy of tubes in cold pilgering. *J. Mater. Process. Technol.* (2016) **231**: 277-287.
[5] Furushima, T. and Manabe, K., Experimental and numerical study on deformation behavior in dieless drawing process of superplastic microtubes. *J. Mater. Process. Technol.* (2007) 191: 59-63.
[6] de Souza Neto, E.A., Peric, D., Dutko and M., Owen, D.R.J. Design of simple low order finite elements for large strain analysis of nearly incompressible solids. Int. J. Solids Struct. (1996) **33** (20-22): 3277-3296.
[7] Manabe, K. and Nishimura, H. Forming loads in tube-flaring with conical punch – Study on noising and flaring of tube V-. J. Jpn. Soc. Technol. Plast. (1983) **24** (264): 47-52, in Japanese.